High-Capacity Optical Wireless Communication by Directed Narrow Beams

Ton Koonen
Eindhoven Hendrik Casimir Institute
Eindhoven Univ. of Technology
Eindhoven, The Netherlands
a.m.j.koonen@tue.nl

***Abstract*—Optical wireless communication (OWC) by means of 2D-steered narrow infrared beams can provide non-shared secure high-capacity connections to individual users, at high user densities. This keynote talk presents an overview of the system architecture and the essential techniques needed for bi-directional broadband indoor/short-reach OWC: simultaneous steering of multiple beams individually, accurately localizing the users and automatically aligning their down- and upstream beams, and capturing the beams with wide-field-of-view broadband receivers in order to avoid tedious alignment. Real-time GbE streaming of high-definition video movies via bi-directional OWC links to individual users has been demonstrated.**

Keywords*— *optical wireless communication, optical beam steering, device localization, optical retro-reflector, photodiode matrix

I. Introduction

Optical wireless communication (OWC) brings a number of distinct advantages beyond radio-based wireless communication (e.g., 4G and 5G mobile, WiFi): the visible and near-IR optical spectrum offer orders of magnitude more bandwidth than the RF spectrum (even in THz frequency bands), crosstalk between users is eliminated by narrow beams and/or opaque walls, the connection is not hampered by electro-magnetic interference nor does it generate EMI, and with narrow beams the energy can be brought only to those places where and when needed, thus yielding high energy efficiency [1]. The small footprints of the beams also support a high user density. By deploying near-IR light such as widely used in fiber-optic communication, relatively high beam powers (10 mW beyond λ=1.4 μm) can be used without eye safety issues, and OWC systems can build on the vast set of mature optical modules already widely used in fiber-optic networks. In contrast with systems using widely diverging beams (such as LiFi systems), systems using narrow (nearly-) collimated beams ensure a good link power budget which enables high-capacity connections with a longer reach.

This keynote paper surveys our research efforts in high-capacity beam-steered optical wireless communication systems using narrow 2D-steered beams for indoor (/short-to-medium range) service delivery. After discussing the indoor OWC network aspects, it summarizes the key techniques required: 2D steering of multiple narrow beams, accurate localization of the OWC receivers, and broadband wide Field-of View (FoV) receivers. These techniques have been validated in a laboratory demonstrator system, showing real-time GbE streaming via bi-directional links of high-definition video movies to individual users.

II. Indoor OWC networks

By using OWC, the opaqueness of the walls which delineates rooms inside a building prevents crosstalk between these rooms which is a major performance- and security-limiting factor when using WiFi. In LiFi systems [2], wide beams are used which have to be shared by multiple users; hence a medium-access control (MAC)protocol is needed and the capacity available per user may fluctuate and even be annihilated by congestion. In OWC systems using 2D-steered narrow beams, however, each user can get his own un-shared beam, thus providing a guaranteed capacity at high privacy, and avoiding the need for MAC protocols, which reduce net capacity and increase system complexity.

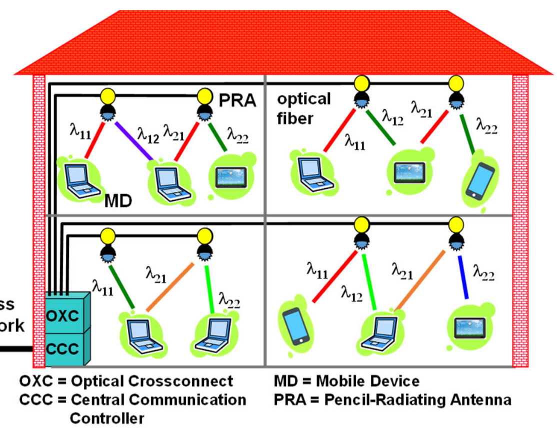

Fig. 1. Indoor OWC system architecture using narrow 2D-steered IR beams

We have proposed the OWC indoor system architecture shown in Fig. 1 (named 'BROWSE – Beam-steered Reconfigurable Optical Wireless System for Energy-efficient communication') [3]. Each room is equipped with pencil-radiating antenna (PRA) modules, mounted at the ceiling, which emit multiple narrow IR beams each directed to a single user. The PRA contains diffractive means which enable to steer each beam by just tuning its wavelength. Preferably wavelengths in C- (1530-1565nm) and L-band (1565-1625nm) are used, i.e., in the eye-safe spectrum beyond 1.4µm and for which numerous mature components already being used in fiber-optic systems are readily available. Moreover, the PRA's diffractive means are passive, which do not need local powering, are not prone to lifetime failures, and enable easy installation. By having multiple PRAs per room, full coverage is obtained and blocking of the line-of-sight from a PRA to a user can be circumvented by selecting an other PRA. The optical data signals are generated in a central communication controller (CCC) site which contains the wavelength-tunable transceivers. These transceivers feed the λ-tuned signals through an optical cross-connect (OXC) unit and the in-building fiber backbone network to the respective PRAs. Each wavelength carries a data signal and also through the diffractive PRA determines the steering of its beam: the wavelength therefore acts as an embedded control channel, and no tedious bookkeeping is needed for tracking which control channel belongs to which data channel. Scaling to more beams (more users) just implies feeding more wavelength channels through the fiber network and installing extra transceiver modules in the CCC, but does not need changes in the PRA modules nor in the fiber network infrastructure, which makes the system's concept easily scalable to many users.

III. Optical beam steering

Various technologies for steering narrow beams have been reported [1]. They may be classified in those using active steering modules, and those using passive modules. Active steering modules may include MEMS micro-mirrors [4] and spatial light modulators (SLMs) [5]; they need a separate control channel for tuning their steering function, and typically each beam needs a separate component which compromises the scalability to larger beam numbers. Passive steering modules encompass diffractive components which direct beams in a direction depending on their wavelength. Scaling to more beams is done by just adding wavelengths. Such diffractive components may be planar diffraction gratings [6], phased array gratings [7], virtually-imaged phased array gratings [8], multiple tilted Bragg gratings in a glass volume [9], polarization gratings [10], etc. The speed with which the beam can be steered is dictated by the speed with which the laser wavelength can be tuned; this can be in the ns to µs regime. For the active steering modules, this is limited to the ms regime, as mechanical or electronic driving restrictions apply.

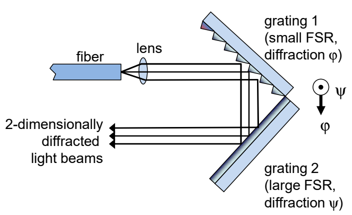

a) 2D beam steering using two crossed diffraction gratings

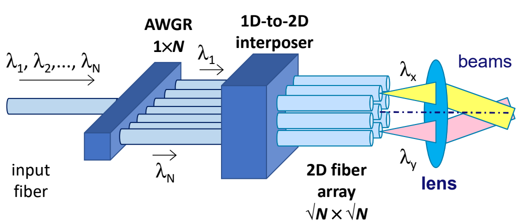

b) 2D beam steering using arrayed waveguide grating router with output ports arranged in 2D fiber array

Fig. 2. Passive 2D beam steering using diffractive components and remote λ-tuning

Fig. 2 shows the two implementations using passive diffractive means we explored for 2D steering multiple beams individually by remotely tuning their wavelengths. As shown in Fig. 2.a, by means of a pair of crossed gratings semi-discrete 2D steering over 5.6°×12.7° has been achieved [11]. Alternatively, as shown in Fig. 2.b, we assembled a robust 2D steering unit by means of a composite C+L$^-$ band arrayed waveguide grating router (AWGR) having 96+48=144 ports (spaced at 50GHz, with a -3dB bandwidth of 35 GHz in C-band and 24GHz in L-band), of which 129 could be incorporated into a 2D fiber matrix, in combination with a *f*=50mm camera lens with aperture *f*/D=0.95. The fiber matrix was defocused with respect to the lens in order to yield slightly diverging beams with a spot size of 12 cm at 2.5 m distance. Thus, by λ-tuning we achieved discrete 2D steering with a complete full-angle coverage of 35°×35° [12]. With a C-band AWGR having 80 output ports, and PAM-4 modulation, we have achieved 112 Gbit/s per beam over 2.5 m reach within the 35GHz -3dB bandwidth per port, yielding an aggregate capacity of 80×112 Gbit/s = 8.96 Tbit/s, with a 17°×17° full-angle coverage [13].

IV. Localization

The steering of narrow optical beams for establishing communication links requires careful localization of the receiver at the link's end. For a bidirectional all-optical OWC system, accurate localization is needed for both the downstream and the upstream links. To enable a connection set-up on the user's initiative, these localization processes should preferably be performed independently from each other.

A. Localization for establishing a downstream link

Steering the narrow beams downstream from the ceiling to the respective users requires acquiring knowledge about the position of each user by localizing him accurately, and updating this knowledge by tracking him when he is moving. Triangulation algorithms may be used at the user side when three or more beacons at the ceiling are provided [14]. The user subsequently needs a return path to transmit his position to the beam steering unit at the ceiling. Alternatively, the user may be localized by means of a camera at the ceiling which can identify him by means of LED tags which emit a unique blinking sequence and are mounted around his receiver's aperture [15][16]. Both these methods require active functions at the user, which consume power.

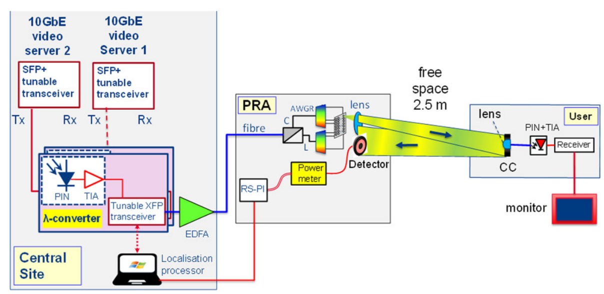

Fig. 3. Passive localization of a user by means of an optical retro-reflector (CC: ring-shaped foil of miniature corner cubes)

In order to minimize this power consumption and maximize the battery life of the user's device, we have explored passive techniques for localizing the user by deploying optical retro-reflector technology [17]. A ring-shaped foil which integrates many miniature corner cubes (CC-s) is mounted around the aperture of the user's receiver. The receiver can then be located by scanning the user area with a beam from the beam steering unit (i.e., a PRA in Fig. 1), and monitoring whether any light of the beam is reflected back to a power monitor next to the beam steerer. As this scanning is done by wavelength tuning, the actual wavelength at the moment that reflected light is detected gives the user's position. This wavelength is subsequently stored and used to set up the downstream link to that user. This auto-calibration process implies that no further bookkeeping is needed to map the user's location to the right wavelength. In contrast, it may be noted that the triangulation method and the camera observation method do need such bookkeeping. As a retro-reflector returns light only in the direction it came from, with our proposed method multiple users can be localized independently. It may also be noted that with the retro-reflector method no parallax errors are incurred, as the same transmitter aperture is used for the scanning beam as well as for the data beams. With the camera observation method, such parallax errors need to be compensated which requires measurement of the distance to each user.

Fig. 3 shows the laboratory setup in which our localization method has been successfully validated [17]. The beam diameter was 10 cm, and the circular foil containing miniature retro-reflecting corner cubes (CC foil) had a diameter of about 5 cm. The scanning of the whole user area (with 129 cells) took about 15 seconds, which is largely consumed by acquisition of the returned reflected light and the control software in LabVIEW.

B. Localization for establishing an upstream link

For bidirectional wireless communication, the return channel may be implemented by a radio link (such as in WiFi systems), or by an optical link as well. In order to preserve OWC's advantages of high privacy and EMI insensitivity, it is preferred to have narrow optical beams in upstream from the users to the common optical receiver at the ceiling. To avoid wavelength-tuning and a high power consumption at the (low-cost, battery-powered) user device, the upstream beam from a laser diode should be emitted at an arbitrary wavelength, and at a medium power level. Such beam should be quite narrow, and fit fully within the aperture of the ceiling's receiver; thus, enough link power budget is created to enable a high data rate. Steering of the upstream beam can be done by mechanical steering (such as moving the laser's fiber with respect to a lens) or by opto-electronic steering (e.g., with an SLM). We opted for mechanical steering by means of stepper motors. These motors need to be activated only when the upstream beam direction is to be altered; thus, power consumption at the (battery-operated) user device is minimized.

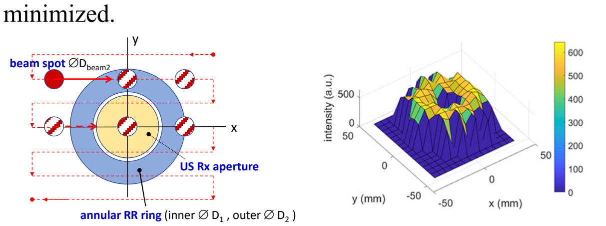

a) scanning the aperture of the upstream receiver

b) monitoring the reflected power from the RR ring

Fig. 4. Aligning the upstream beam by the CoG algorithm

For aligning the upstream beam, typically a pre-existing downstream path is needed for monitoring whether good alignment has been reached. When the connection setup is to be initiated upon request by the user, such downstream path may not exist yet. Hence, we have proposed an optical retro-reflection method in combination with a hole-seeking algorithm [19][20]. It uses a ring of miniature retro-reflectors (RR-s), made of a CC foil similar as used for the downstream localization. This RR ring with outer diameter ∅62 mm and inner diameter ∅25 mm is mounted tightly around the ∅25 mm aperture of the upstream receiver at the ceiling, positioned next to the PRA. Next to the upstream transmitter at the user, a power monitoring photodiode is mounted to monitor the reflected light. As the upstream beam's footprint (of ∅15 mm in our system) is smaller than the ∅25 mm aperture of the upstream receiver, the monitored power when scanning with the upstream beam shows a donut intensity profile (see Fig. 4). By calculating the center of this donut according to a center-of-gravity algorithm, the center of the aperture of the upstream receiver is localized and the corresponding beam's direction is determined. Subsequently, the upstream data transmission along this same beam is started. This localization process is self-aligned; no additional calibration is needed for matching the localization to the beam's direction.

The configuration of our bidirectional OWC system demonstrator is shown in Fig. 5. The upstream beam alignment time is less than 10 seconds, and is mainly limited by the speed of the stepper motors for the mechanical steering.

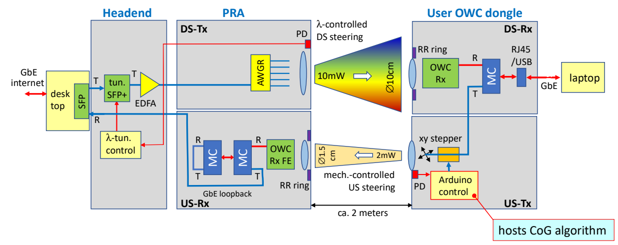

Fig. 5. Bidirectional all-optical wireless system for GbE full-duplex communication

V. BROADBAND OPTICAL RECEIVER WITH WIDE FOV

Capturing as much as possible of an optical beam while minimizing the efforts to align the receiver is a key challenge in optical wireless transmission. The receiver should therefore have a large aperture and wide Field-of-View (FoV), and preferably (in particular at the user side) should be compact, have low complexity, and consume little power. Wide FoV solutions have been reported by receivers using non-imaging optics (such as compound parabolic concentrators, CPC-s [21]), angular diversity receivers (ADR-s) using multiple branches of photodiodes (PD-s) and transimpedance amplifiers (TIA-s) [22][23], receivers using etendue enlargement by wavelength conversion in phosphorescent slab waveguide [24] or fiber [25], and receivers using photonic integration of a large surface grating coupler (SGC) or multiple SGC-s plus waveguide combiner in conjunction with a waveguide-fed UTC photodiode [26].

We have proposed a receiver architecture using a 2D matrix of photodiodes which has only a single outlet, needs only a single TIA, and thus has low complexity and low power consumption; see Fig. 6. Initially, this concept was proposed using a quad photodiode [27], and subsequently extended into a scalable $N \times N$ photodiode matrix [28]. Such receiver can have a bandwidth and noise performance equal to a receiver employing just a single high-speed photodiode, while it has a significantly larger aperture and FoV [27][28]. Uneven illumination of the photodiodes in the matrix may yield unequal bias voltages across these photodiodes which can affect their bandwidth. By adding shunting resistors as shown in Fig. 6.a, these voltage unbalances are minimized, with no impact on the receiver's bandwidth [28].

We built a receiver deploying a wired 4×4 matrix of ∅150 µm photodiodes (Fig. 6.b) and combined it with a TIA having 670 MHz bandwidth and a Fresnel lens with 50 mm diameter and focal length f=10 mm (Fig. 6.c). We successfully demonstrated GbE (1.25Gbit/s) operation at BER<10^{-9} within a FoV of ±10° (half angle) at a reach of 2 m.

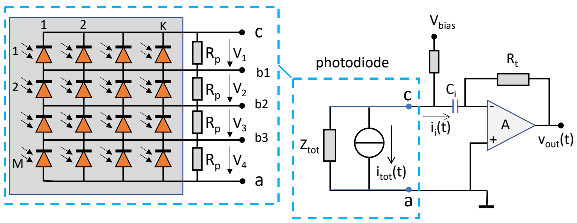

a) OWC receiver architecture

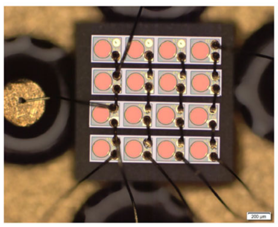

b) 4×4 PD matrix

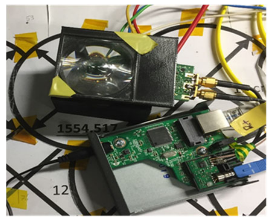

c) OWC receiver with Fresnel lens ∅50 mm, *f*=10mm

Fig. 6. OWC receiver with 2D matrix of photodiodes

Fig. 7 shows the FoV improvement which can be obtained by applying a 4×4 PD matrix as compared to the FoV when using a single PD. By increasing the defocusing, i.e., putting the photodiode matrix (or single PD) closer to the lens, beyond its focal plane, the beam's spot projected onto the matrix (/ single PD) is enlarged and the FoV is increased; this is accompanied by a reduced equivalent coupling factor T_{eq} of the beam to the matrix, however. Hence, the FoV which can be obtained is a compromise with the T_{eq} which is needed to achieve a sufficient link power budget. To assess this compromise, we made a theoretical analysis (assuming a uniform beam and ideal thin lens; see [28]) as well as we did ray tracing (with a self-built MATLAB program) with 25117 rays traced per FoV step of 0.2 deg., assuming a Gaussian beam and Fresnel lens with large D/*f*-number. Fig. 7.a shows the results calculated for the downstream link, where the beam has a relatively large footprint of 100 mm in order to cover a larger user area and hence a large-aperture Fresnel lens of ∅50 mm with *f*=10 mm is used at the user's downstream receiver. Fig. 7.b shows the results for the upstream link, where the beam is narrower with footprint ∅15 mm to fit within the ∅25 mm aperture of the Fresnel lens with *f*=5 mm at the ceiling's upstream receiver. The results obtained by the extensive ray tracing for the Gaussian beam profile and Fresnel lens (a thin Fresnel collector lens model is adopted) match fairly well with the results obtained from the theoretical analysis assuming a uniform beam profile and ideal aberration-free thin lens [28]. This matching is somewhat better for the downstream case than for the upstream one, as in the downstream case only part of the Gaussian beam is admitted by the lens aperture and hence the deviation of the Gaussian profile from the uniform profile is less noticeable. For both the downstream and the upstream case, it can be noted that at the same beam-to-photodiode coupling factor T_{eq} the obtainable FoV when using the PD matrix concept is significantly larger than when using a single photodiode. According to the theoretical analysis, the obtainable FoV also is inversely proportional to the lens' focal length *f*. For downstream, the launched power per beam is about 10 dBm; with a receiver sensitivity of -20 dBm for GbE operation, a T_{eq}=-30 dB is required. Fig. 7.a shows that a FoV≈±13 deg. (half-angle) can be obtained. For upstream, about 2 dBm is launched, hence a FoV≈±18 deg. is achievable according to Fig. 7.b. Note that also the smaller lens focal length yields the higher FoV.

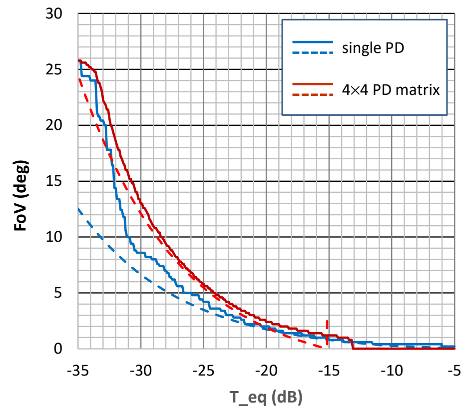

a) Downstream: beam ∅100 mm, lens ∅50 mm with *f*=10 mm

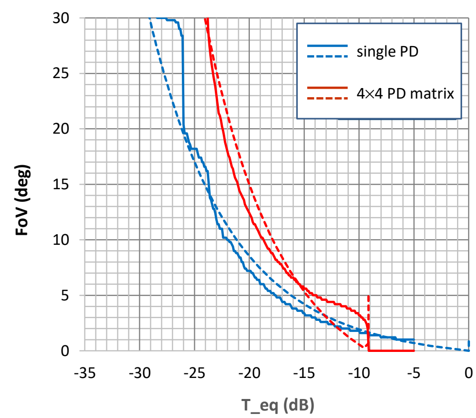

b) Upstream: beam ∅15 mm, lens ∅25 mm with *f*=5 mm

Fig. 7. FoV vs. beam-to-PD coupling T_{eq} for a single ∅150µm PD and for a 4×4 matrix of ∅150µm PDs spaced at 17µm (solid curves: by ray tracing for Gaussian beam and with Fresnel lens; dashed curves: by theoretical analysis, for uniform beam and ideal thin lens)

The impact on the FoV of scaling the PD matrix to other *N*×*N* dimensions has been analyzed by numerical integration for the case of a Gaussian beam profile and an ideal aberration-free thin lens. For downstream, under the same assumptions as used for Fig. 7, at a required T_{eq}=-30 dB according to Fig. 8.a the attainable FoV≈±7.5 deg. for a single PD and grows from ±11 deg. to ± 21 deg. when the PD matrix is enlarged from 2×2 to 8×8. For upstream, with a required T_{eq}=-22 dB, an FoV≈±11 deg. is attainable for a single PD and an FoV growing from ±11 deg. to ±26 deg. when the PD matrix size increases from 2×2 to 8×8 deg. Upscaling the PD matrix thus increases the FoV performance, but this FoV increase becomes less significant at larger matrix sizes. The scalability of our PD matrix concept has been validated at high data rates; 25Gbit/s NRZ modulated transmission over 20 m has been demonstrated with a 20×20 matrix of 30 µm PD-s [29].

When compared to an ADR, it can be shown that our proposed PD matrix receiver has the same bandwidth and a better SNR. See Fig. 9: assuming that thermal receiver noise dominates, for the SNR at the output of the PD matrix receiver we find $\frac{S_{out}}{N_{out}} = \frac{(N\,\bar{a}\,R\,P_O)^2}{F_1 \cdot i_{th}^2}$ whereas for the ADR with an equal amount of N^2 PD-s we find $\frac{S_{out}}{N_{out}} = \frac{(N\,\bar{a}\,R\,P_0)^2}{F_1 \cdot F_2 \cdot i_{th}^2}$ which is $1/F_2$ worse (F_1 and F_2 are the noise figures (>1) of the TIA and the summation amplifier, respectively; $\bar{a}$ is the average fraction of the beam's power P_0 which is captured by a PD, R is the responsivity of a PD, and i_{th}^2 is the thermal noise input power of the TIA). Moreover, the PD matrix receiver needs only a single TIA, thus is less complex and consumes less power.

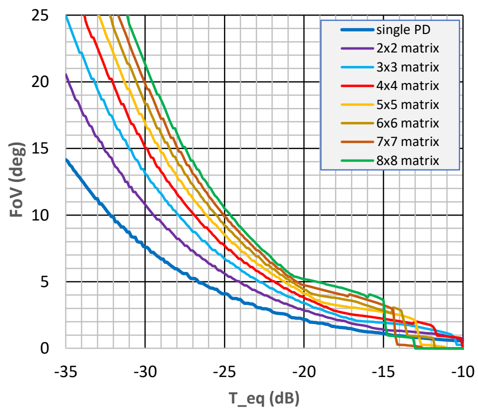

a) downstream (Gaussian beam ∅100 mm, thin lens ∅50 mm, f=10 mm)

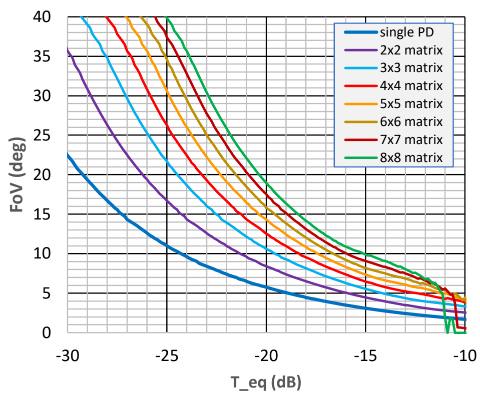

b) upstream (Gaussian beam ∅15 mm, thin lens ∅25 mm, f=5 mm)

Fig. 8. Impact of scaling the PD matrix on the FoV

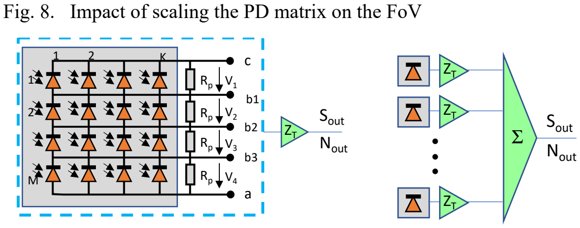

a) $N \times N$ PD matrix receiver b) ADR with N^2 PD-s

Fig. 9. Comparing the PD matrix receiver with an ADR

VI. Bi-directional OWC system demonstrator

Many beam-steered bidirectional OWC systems reported used optical communication only for downstream, and radio means for upstream. To preserve the key benefits of beam-steered OWC, notably dense high-capacity individual connectivity with high privacy and EMI immunity, in upstream optical beams should be used also. By recovering the optical carrier from the downstream beam by means of an SOA operating in gain-saturation and modulating this carrier with the upstream data, a full-duplex all-optical wireless link has been demonstrated [18]. This approach had a narrow FoV and requires a limited extinction ratio of the downstream signal, however, which reduces the downstream link budget and requires very careful alignment of the user's OWC module.

In our extended laboratory system, we have shown successfully GbE full-duplex bidirectional all-optical wireless communication with automatic alignment of the downstream beams and the upstream beams, as described in section IV. The system architecture is shown in Fig. 5, and its actual implementation in Fig. 10 [19][20]. The PRA site featuring the downstream transmitter (DS-Tx) and upstream receiver (US-Rx) surrounded by the RR ring aiding the upstream beam alignment is shown in Fig. 11. Fig. 12 shows the user site, including the upstream transmitter (US-Tx) equipped with stepper motors for the upstream beam alignment and the downstream receiver (DS-Rx) with the RR ring for the automated downstream beam alignment. Performance measurements with Iperf in TCP tests showed 940 Mbit/s downstream and 939 Mbit/s upstream transmission without packet loss, within a reach of about 2 m and with a FoV of ±10° (half-angle). With that, we demonstrated live GbE streaming of high-definition video movies to a laptop, connected via the user OWC dongle through an RJ45 interface.

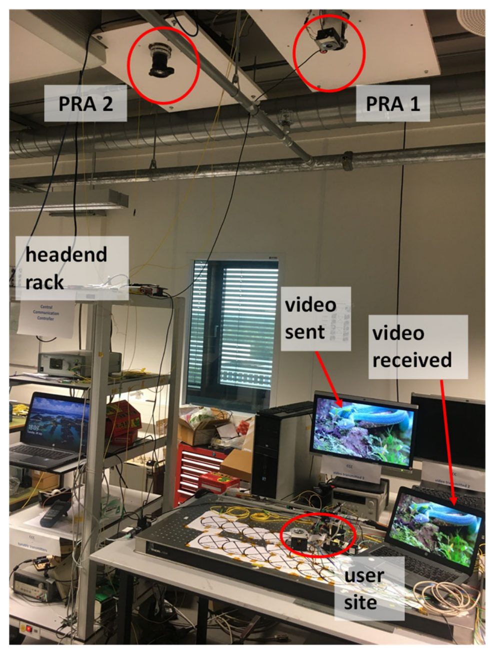

Fig. 10. Bi-directional OWC system for beam-steered GbE transmission

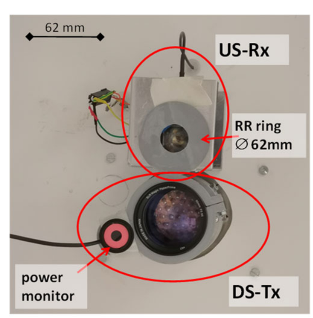

Fig. 11. PRA site (at ceiling)

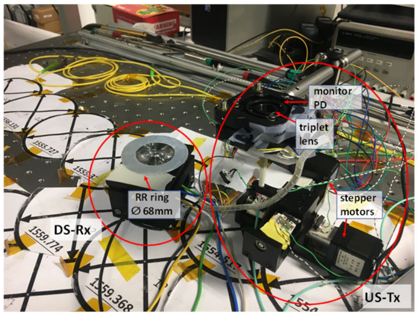

Fig. 12. User site

VII. Concluding Remarks

By deploying 2D-steered narrow optical beams, a laboratory optical wireless communication system for indoor delivery of broadband services to closely spaced individual users has been designed and built. Using optical retro-reflector techniques, automatic and auto-calibrated alignment of downstream and upstream beams was achieved. We successfully demonstrated live streaming of GbE high-definition video movies to laptop computers individually.

The author is grateful for support in the experimental work by Dr. Ketema Mekonnen and Mr. Frans Huijskens, and for valuable discussions with his colleagues, in particular Dr. Eduward Tangdiongga and Dr. Zizheng Cao. Funding from the European Research Council in the Advanced Grant BROWSE and Proof of Concept BROWSE+ programs is gratefully acknowledged, as well as funding by the Dutch Scientific Research Organization in the Nanophotonics Gravitation program.

References

[1] A.M.J. Koonen, "Indoor optical wireless systems: Technology, trends, and applications," *J. Lightw. Technol.*, vol. 36, no. 8, pp. 1459–1467, Apr. 2018, (doi: 10.1109/JLT.2017.2787614.)

[2] H. Haas, L. Yin, Y. Wang, C, Chen, 2016. "What is LiFi?," *J. Lightw. Technol.*, 2016, vol. 34, no. 6, pp. 1533-1544. (doi: https://doi.org/10.1109/JLT.2015.2510021).

[3] A.M.J. Koonen et al., "Ultra-high capacity wireless communication by means of steered narrow optical beams," *Philos. Trans. Roy. Soc. A*, 2020, art. no. 19 (doi: http://dx.doi.org/10.1098/rsta.2019.0192).

[4] K. Wang, A. Nirmalathas, C. Lim, K. Alameh, E. Skafidas, "Full duplex gigabit indoor optical wireless communication system with CAP modulation," *Photon. Technol. Lett.*, vol. 28, no. 7, pp. 790–793, Apr. 2016.

[5] A. Gomez, K. Shi, C. Quintana, M. Sato, G. Faulkner, B.C. Thomsen, D. C. O'Brien, "Beyond 100-Gb/s indoor wide field-of-view optical wireless communications," *Phot. Technol. Lett.*, vol. 27, no. 4, Feb. 2015, pp. 367-370.

[6] C.W. Oh, E. Tangdiongga, and A.M.J. Koonen, "Steerable pencil beams for multi-Gbps indoor optical wireless communication," *Optics Letters*, vol. 39, no. 18, Sep. 2014, pp. 5427-5430.

[7] J.K. Doylend, M.J.R. Heck, J.T. Bovington, J.D. Peters, L.A. Coldren, and J.E. Bowers, T. Chan, E. Myslivets, and J.E. Ford, "2-Dimensional beamsteering using dispersive deflectors and wavelength tuning," *Optics Express*, vol. 16, no. 19, Sep. 2008, p. 14617-14628.

[8] T. Chan, E. Myslivets, and J.E. Ford, "2-Dimensional beamsteering using dispersive deflectors and wavelength tuning," *Optics Express*, vol. 16, no. 19, Sep. 2008, p. 14617-14628.

[9] Z. Yaqoob, M.A. Arain, and N.A. Riza, "High-speed two-dimensional laser scanner based on Bragg gratings stored in photothermorefractive glass," *Applied Optics*, vol. 42, no. 26, Sep. 2003, p. 5251-5262.

[10] C. Hoy, J. Stockley, J. Shane, K. Kluttz, D. McKnight and S. Serati, "Non-Mechanical Beam Steering with Polarization Gratings: A Review," *MDPI Crystals*, 2021, 11, 361 (21 pp.) (doi: https://doi.org/10.3390/cryst11040361)

[11] A.M.J. Koonen, C. W. Oh, K. Mekonnen, Z. Cao, and E. Tangdiongga, "Ultra-high capacity indoor optical wireless communication using 2D-steered pencil beams," *J. Lightw. Technol.*, vol. 34, no. 20, pp. 4802–4809, Oct. 2016.

[12] A.M.J. Koonen, F. Gomez-Agis, F.M. Huijskens, and K.A. Mekonnen, "High-capacity optical wireless communication using two-dimensional IR beam steering," *J. Lightw. Technol.*, vol. 36, no. 19, pp. 4486–4493, Oct. 2018.

[13] F. Gomez-Agis, S.P. van der Heide, C.M. Okonkwo, E. Tangdiongga, and A.M.J. Koonen, "112 Gbit/s transmission in a 2D beam steering AWG-based optical wireless communication system," *Proc. ECOC2017*, Göteborg, Sweden, Sep. 2017, Paper Th.2.B.1.

[14] H. Liu, H. Darabi, P. Banerjee, J. Liu, "Survey of Wireless Indoor Positioning Techniques and Systems," *IEEE Trans. on Systems, Man, and Cybernetics*, vol. 37, no. 6, pp. 1067-1080, Nov. 2007.

[15] A. Gomez, K. Shi, C. Quintana, G. Faulkner, B.C. Thomsen, D. O'Brien, "A 50 Gb/s transparent indoor optical wireless communications link with an integrated localization and tracking system," *J. Lightw. Technol.*, vol. 34, no. 10, pp. 2510-2517, May 2016.

[16] N. Q. Pham, K. Mekonnen, E. Tangdiongga, A. Mefleh, T. Koonen, "User Localization and Upstream Signaling for Beam-Steered Infrared Light Communication System," *Phot. Technol. Lett.*, vol. 33, no. 11, pp. 545–548, 2021.

[17] A.M.J. Koonen, K.A. Mekonnen , F.M. Huijskens , N.-Q. Pham, Z. Cao, E. Tangdiongga , "Fully passive user localization for beam-steered high-capacity optical wireless communication system," *J. Lightw. Technol.*, vol. 38, no. 10, pp. 2842-2848, May 2020.

[18] C.W. Oh, Z. Cao, K.A. Mekonnen, E. Tangdiongga, A.M.J. Koonen, "Low-crosstalk full-duplex all-optical indoor wireless transmission with carrier recovery," Phot. Technol. Lett., vol. 29, no. 6, Mar. 2017, pp. 539-542.

[19] A.M.J. Koonen, K. A. Mekonnen, F.M. Huijskens, E. Tangdiongga, "Bi-directional all-optical wireless communication system with optical beam steering and automatic self-alignment," *Proc. ECOC2022*, Basel, Sep. 18-22, paper Tu4F.1.

[20] A.M.J. Koonen, K.A. Mekonnen, F.M. Huijskens, E. Tangdiongga, "Bi-directional all-optical wireless gigabit Ethernet communication system using automatic self-aligned beam steering," *J. Lightw. Technol.*, Dec. 2022, 9 pp., (early access at https://doi.org/10.1109/JLT.2022.3231438).

[21] K. Wang, A. Nirmalathas, C. Lim, K. Alameh, and E. Skafidas, "Full duplex gigabit indoor optical wireless communication system with CAP modulation," *Photon. Technol. Lett.*, vol. 28, no. 7, pp. 790–793, Apr. 2016.

[22] J. Zeng, V. Joyner, J. Liao, S. Deng, Z. Huang, "A 5Gb/s 7-channel current-mode imaging receiver front-end for free-space optical MIMO," *Proc. IEEE MWSCAS2009*, Cancun, pp. 148-151.

[23] Z. Zeng, M. Dehghani Soltani, M. Safari, H. Haas, "Angle Diversity Receiver in LiFi cellular networks," *Proc. ICC2019*, Shanghai, July 2019.

[24] S. Collins, D. C. O'Brien, [24][25]and A. Watt, "High gain, wide field of view concentrator for optical communications," *Opt. Lett.*, vol. 39, no. 7, Apr. 2014, p. 1756-1759.

[25] A. Riaz and S. Collins, "A wide field of view VLC receiver for smartphones," *Proc. ECOC2020*, Brussels, Dec. 2020, paper Tu2G.4.

[26] Z. Cao, L. Shen, Y. Jiao, X. Zhao, A. M. J. Koonen, "200 Gbps OOK transmission over an indoor optical wireless link enabled by an integrated cascaded aperture optical receiver," *Proc. OFC2017*, Los Angeles, post-deadline paper Th5A.6.

[27] A.M.J. Koonen, K. A. Mekonnen, F. M. Huijskens, Z. Cao, E. Tangdiongga, "Novel Broadband OWC Receiver with Large Aperture and Wide Field of View", *Proc. ECOC2020*, Brussels, Dec. 2020, paper Tu2G.6.

[28] A.M.J. Koonen, K.A. Mekonnen, Z. Cao, F.M. Huijskens, N.-Q. Pham, E. Tangdiongga, "Beam-steered optical wireless communication for industry 4.0", *IEEE J. of Sel. Topics in Quantum Electron.*, Vol. 27, No. 6, Nov./Dec. 2021, art. 6000510 (10 pp.). (doi: https://doi.org/10.1109/JSTQE.2021.3092837).

[29] T. Umewaza, AQ. Matsumoto, K. Akahane, A. Kanno, N. Yamamoto, "400-pixel high-speed photodetector for high optical alignment robustness FSO receiver," *Proc. OFC 2022*, San Diego, Mar. 2022, paper M4I.3.